

Heat Transfer Studies on Structured Metal Sheets

Josef Egert* and Karel Fraňa

Department of Power Engineering Equipment, Faculty of Mechanical Engineering, Technical University of Liberec, Czech Republic

Sylvio Simon and Steffen Wichmann

Fakultät Maschinenbau, Elektrotechnik und Wirtschaftsingenieurwesen, Brandenburg University of Technology Cottbus-Senftenberg, Germany

* Corresponding author. E-mail: josef.egert@tul.cz DOI: 10.14416/j.ijast.2016.05.002

Received: 21 April 2016; Accepted: 15 May 2016; Published online: 31 May 2016

© 2016 King Mongkut's University of Technology North Bangkok. All Rights Reserved.

Abstract

Unsteady turbulent airflow in a parallel way with a plain and a hexagonal sheet was analyzed numerically and experimentally in order to determine the heat transfer intensity between surfaces of sheets and surrounding airflow. To obtain experimental results for validation of numerical simulations, a measurement facility, composed from aerodynamics tunnel and wire heater, was designed and constructed. The temperature on the sheets was chosen to observe the effects of different surface structures, airflow conditions and input heat power. Results provided by numerical simulations showed good conformity with experimental results. For investigated cases the hexagonal sheet achieved significantly higher heat transfer intensity and lower surface temperature than the plain sheet under the same conditions.

Keywords: Structured metal Sheet, Heat transfer, CFD, Wind tunnel

1 Introduction

This article deals with experimental and numerical analysis of heat transfer on metal sheets with different surface structures. With certain structure created on the plain sheet it is easily possible to improve its mechanical properties [1]. This enhancement was used in various technical applications for example referred in [1], [2]. Furthermore, from the point of the heat transfer mechanism, the structured surfaces intensified the convection heat transfer rate due to higher surface area and the suitable flow behavior around the structured metal sheets as referred in [3], [4]. This ability allows to use these structured sheets in applications where the intensified convection heat transfer is needed, typically in the heat exchangers

and also in the heat (thermal) shields. There are many studies dealing with the heat exchangers design regarding to the structured sheets of the heat exchanges [3]–[5]. However, this paper focuses on heat shield application which is typically used in automotive. The function of heat shields is to create a barrier between parts which should stay cool even if they are affected by the high temperature radiation from the heat sources. The surface of the heat shield reflects majority of incoming radiative heat part. Remaining part is absorbed by the heat shield. Then the absorbed heat is transferred to the surrounding air by convection or by back radiation. Heat shields are typically placed inside the exhaust tunnel on the car chassis. It prevents the heat coming from the exhaust to penetrate into the car interior and causes uncomfortable climate

Please cite this article as: J. Egert, K. Fraňa, S. Simon, and S. Wichmann, "Heat transfer studies on structured metal sheets," *KMUTNB Int J Appl Sci Technol*, vol. 9, no. 3, pp. 189–196, July–Sept. 2016.



Figure 1: The example of heat shield part [6].

conditions for passengers. Another placement is in the car engine compartment on the interface with the cabin. The reason is also to prevent the heat entering the car interior. In sport cars the heatshields are also used for covering certain engine parts which should stay cool. For heat shield application it is important that the material has high reflectivity, high resistivity against corrosion, high scratch resistance and the possibility to be formed to a required shape (for example an exhaust tunnel). The example of a heat shield is shown in Figure 1.

In this study the sheet with hexagonal structure was tested and results were compared with the results provided by the sheet with plain surface. Tested sheet with hexagonal structure is shown in Figure 2 and Figure 3. Its mechanical properties were studied in previous studies [7], [8].

The chapter “Measurement facility” introduces the experimental device which was used for experimental investigations. This device was constructed completely for the purpose of the measurement. The chapter “Numerical model” summarizes basic parameters used for numerical calculations. The preliminary results and conclusions from [3] were adopted for the appropriate choice of the main numerical parameters. Chapter “Theoretical equations and parameters” briefly describes used non-dimensional parameters and equations adopted for the heat transfer calculations. Chapter “Results” discusses the main obtained results and validations of the numerical results gained by experiments.

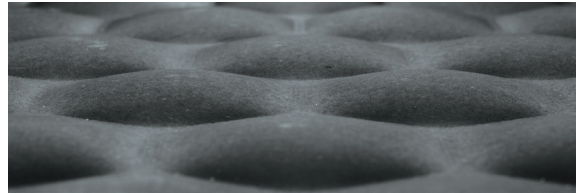


Figure 2: Hexagonal structure sheet–side view.

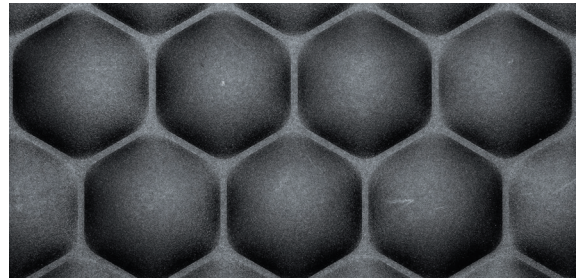


Figure 3: Hexagonal structure sheet–top view.

2 Measurement Facility

The combination of an open aerodynamic tunnel with a resistive wire heater located inside the isolated box was used for the experiment. The sketch of the experimental model can be seen in Figure 4. At the inlet of the model, there is a rectangular contraction part [1] which sucks the surrounding air and leads it into the tunnel body [2]. Inlet airflow speed and temperature was measured by a hot wire anemometry sensor [3]. Measured metal sheet [4] was located near the bottom side of the test section. One part of the sheet was cooled by the airflow and the other part was heated by the convection from the hot air and by the heat radiation. The global temperature field on the sheet surface was measured by the infrared camera [5] placed inside the vertical part of the tunnel [6]. The instantaneous temperature on the sheet’s surface was also measured by a thermocouple [7] which was fixed on particular position. The heated airflow left the measurement facility through the diffusor part [8] and the axial ventilator [9]. In order to minimize heat losses, the heating box was isolated by a polystyrene layer [10], mineral cotton layer [11], calcium-silicate layer [12] and aluminum foil [13]. Resistive wire heater [14] was placed in the bottom side of the inner heating box. The supplied heat and the power consumption of the heater was measured by a wattmeter [15]. The temperature inside the heat box was measured with the thermocouple [16]. To measure

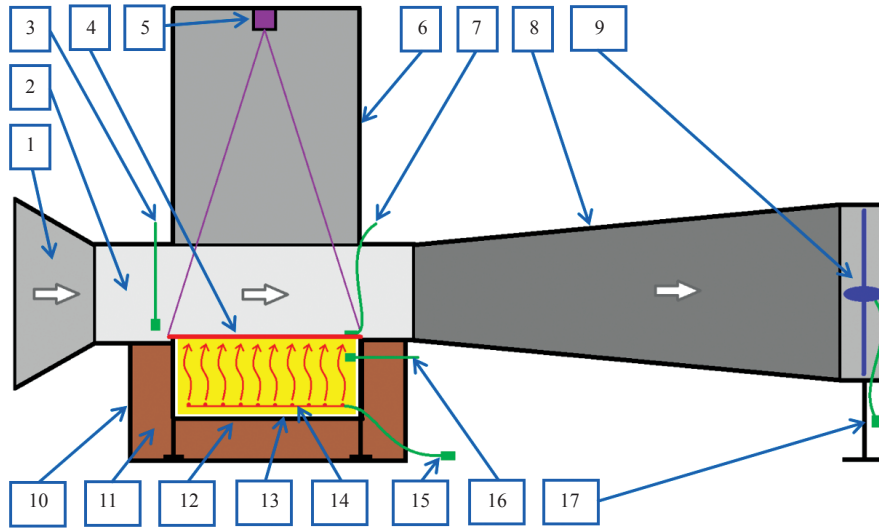


Figure 4: Sketch of the measurement facility.



Figure 5: Test section–front view.



Figure 6: Heating box.

different flow regimes, the ventilator rotational speed was controlled by the speed rotation regulator [17]. Samples from the experimental model are shown in Figure 5 and Figure 6.

3 Measurement Description

Tested sheets were measured in the heating power range from 100 W to 500 W and Reynolds numbers varied from 10000 to 145000. The Reynolds number range was given by the airflow speed which was limited by the ventilator's power. Furthermore, the range of the heating power was limited by the infrared camera

range used for temperature measurements. For every investigated state the infrared images were taken and the average and maximum temperature of the sheet's surface were determined. Also the ambient temperature and heating box internal temperature were recorded.

Separately, the temperature on the sheet surface in one particular position was measured by a thermocouple. This temperature value was used for calibrations in order to identify the real emissivity coefficient further used for settings of thermocamera. By comparison

between temperatures measured on the sheet's surfaces by the thermocouple and a thermocamera the emissivity was set to value 0.9.

4 Numerical Model

Significant parts of this study were numerical simulations. The ANSYS DesignModeler and the ANSYS Meshing were used for geometries and grid preparations and the ANSYS Fluent in version 17 was used as a solver for calculations. The computational domain consisted of simple rectangular shapes with structured sheet imprinted to the bottom side. Numerical grids were generated with the Cut Cell method with prismatic layers near sheet surfaces. For hexagonal sheets the symmetry boundary condition was used in the middle of the domain.

Numerical simulations were performed as steady solution with the turbulent model $k-\omega$ SST. The medium was set to be an incompressible ideal gas. Boundary conditions were set as follows: inlet–velocity inlet, outlet–pressure outlet, side wall and top wall–walls with constant temperatures, symmetry–symmetry for structured sheets or walls with a constant temperature for plain sheets, sheet surfaces–walls with convection and conduction inside the metal sheets.

5 Theoretical Equations and Parameters

The Reynolds number was applied as a relevant number and it takes a form as

$$Re = \frac{cL}{\nu} \quad (1)$$

where c [m/s] is the airflow velocity, L [m] is characteristic length and ν [m²/s] is a kinematic viscosity of the surrounding air. The characteristic length is defined as equivalent hydraulic diameter

$$L = \frac{4A}{O} \quad (2)$$

where A [m²] is a tunnel cross section and O [m] is circumference of the tunnel cross-section. To compare results with other studies every physical quantity was normalized. For temperature evaluations the normalization to ambient temperature was used. The normalized temperature is defined as

$$T_N = \frac{T}{T^*} \quad (3)$$

where T [°C] is measured temperature and T^* [°C] is ambient temperature during the measurement. Assuming, that the lab space was large enough, the heat power could not influence the internal temperature in the surroundings. It means that this ambient temperature corresponded to the temperature of the surroundings. The heat transferred throughout the sheets can be expressed as follows

$$\underline{Q}_S = \underline{Q}_C - \underline{Q}_Z \quad (4)$$

where \underline{Q}_C [W] is the overall heat generated by the heating wire and \underline{Q}_Z [W] is the heat loss through heating box walls. The heat loss is determined by heating box materials. The transferred heat from the sheet surfaces to the surrounding airflow is defined as

$$\underline{Q}_S = \alpha(t - t_s)S \quad (5)$$

where α [W/(m²K)] is the convective heat transfer coefficient, t [K] is average sheet temperature, t_s [K] is ambient temperature and S [m²] is the sheet area. In case of convection, the heat transfer intensity is commonly express by the Nusselt number, which takes a form as

$$Nu = \frac{\alpha l}{\lambda} \quad (6)$$

Where l [m] is the sheet length and λ [W/(mK)] is the thermal conductivity of the surrounding air. The Nusselt numbers, in this study investigated cases, with the power heating of 300W were in the range from 600 to 1400 for plain sheets.

6 Results

The dependence of temperatures on the surfaces of sheets under various airflow and heat conditions was investigated experimentally. Results are shown in Figure 7 and Figure 8. On the horizontal axis there is Reynolds number as expression for inlet airflow conditions. On the vertical axis there is normalized temperature on the surfaces of sheets. Average values of temperatures on the surfaces of sheets were considered for case in Figure 7 and maximum values

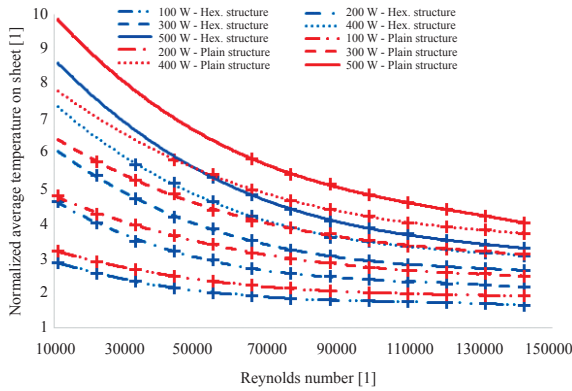


Figure 7: Comparison of normalized average temperature on hexagonal and plain sheets under various airflow and heat output conditions.

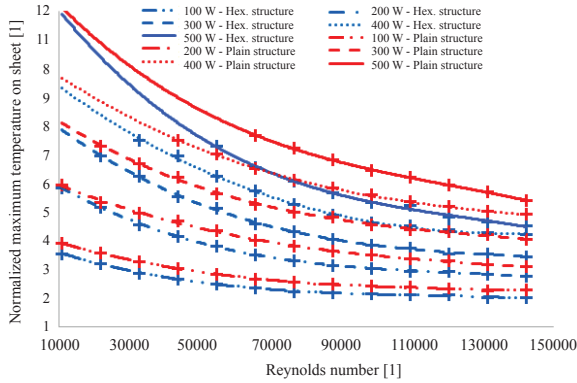


Figure 8: Comparison of normalized maximum temperature on hexagonal and plain sheets under various airflow and heat output conditions.

of the temperatures were considered for case in Figure 8. For both types of temperature evaluations, temperatures decreased with Reynolds number growth. This relationship between temperatures on sheets and surrounding airflow conditions had a non-linear character. Experimental investigations proved that the sheets with hexagonal structure provided more intensive heat transfer than the plain sheets and consequently, surface temperatures at structured sheets were lower than at the plain ones. This effect was more obvious at higher heating power and higher Reynolds numbers and it is in agreement with [9]. For the lower Reynolds number, the measured temperatures on hexagonal sheets were closed to temperatures on plain sheets. Results provided by experiments were

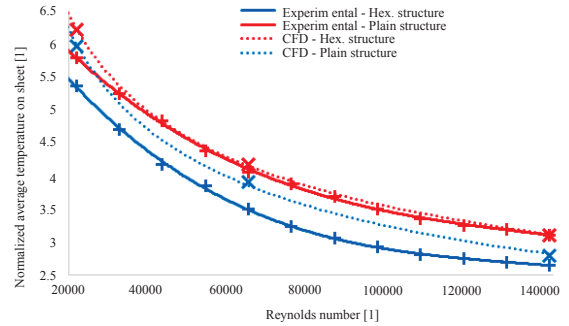


Figure 9: Comparison of results from experimental measurement and computational fluid dynamics (CFD) on normalized average temperature on hexagonal and plain sheets under various airflow conditions.

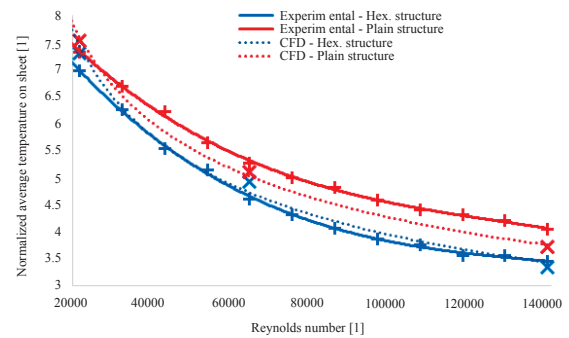


Figure 10: Comparison of results from experimental measurement and computational fluid dynamics (CFD) on normalized maximum temperature on hexagonal and plain sheets under various airflow conditions.

compared with numerical simulations. For comparison three states were considered: 300 W – Re = 22 000, 300 W – Re = 65 000 and 300 W – Re = 142 000. Figure 9 and Figure 10 show the comparison between numerical and experimental results. For average temperatures, the CFD results are in good agreement with experimental results for the plain sheet. For hexagonal sheet the CFD values are higher than measured ones. For maximum temperatures, the CFD results are in good agreement with experimental results for the hexagonal sheet. For plain sheet the CFD values are lower than measured ones. Possible reasons for these deviations are: 1) Inaccuracy of inlet velocity profile used for numerical simulations. 2) Inaccuracy of inlet heat profile used for numerical simulations.

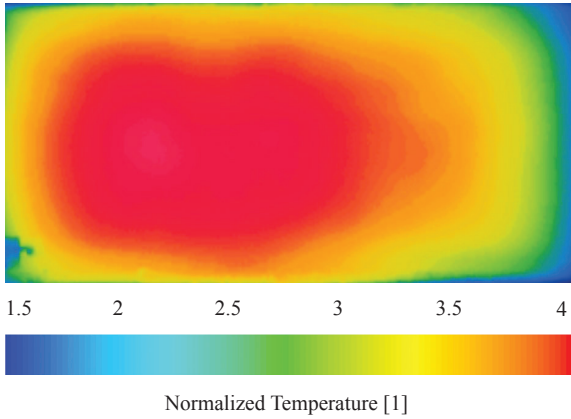


Figure 11: Temperature field on plain sheet surface – experimental measurement.

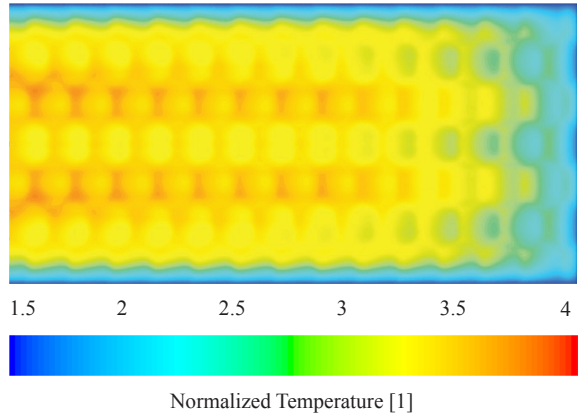


Figure 14: Temperature field on hexagonal sheet surface – numerical simulation.

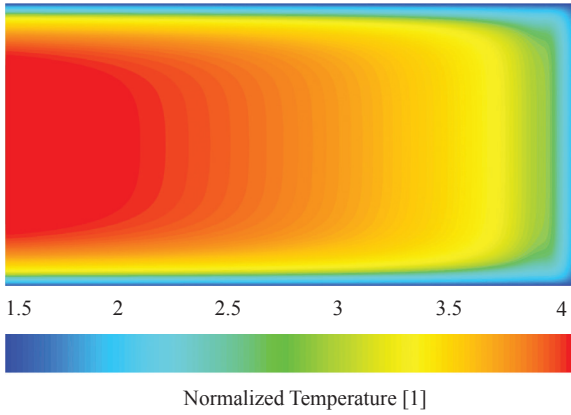


Figure 12: Temperature field on plain sheet surface – numerical simulation.

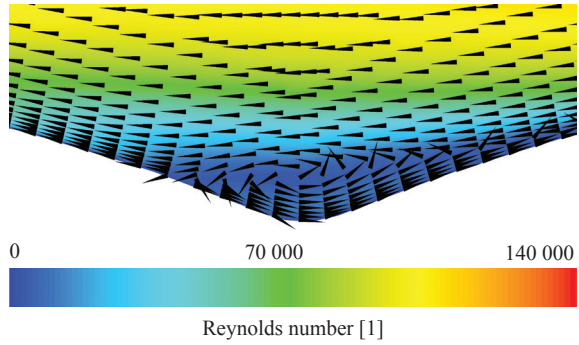


Figure 15: Velocity field on area between two hexagons – numerical simulation (cut parallel to flow direction).

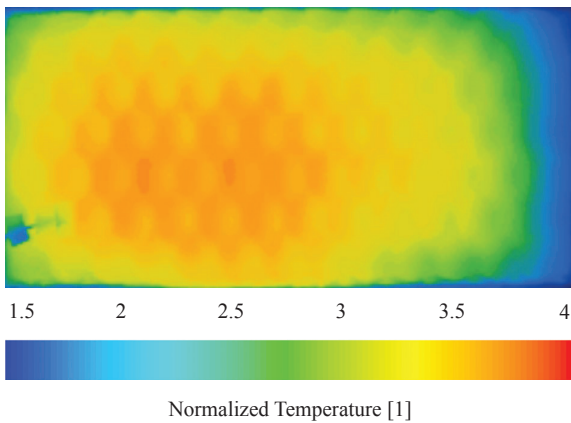


Figure 13: Temperature field on hexagonal sheet surface – experimental measurement.

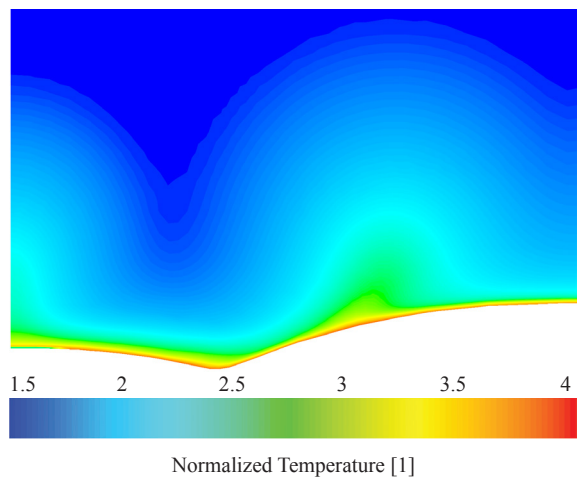


Figure 16: Temperature field on hexagonal sheet outlet face (cut crosswise to flow direction).

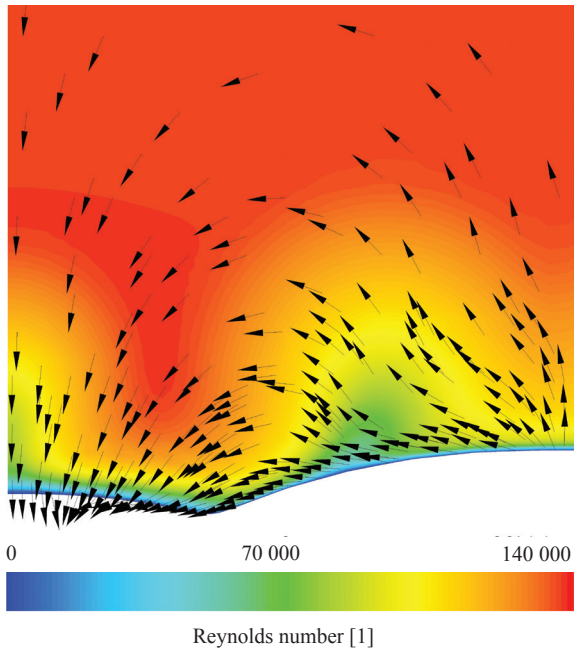


Figure 17: Velocity field on hexagonal sheet outlet face (cut crosswise to flow direction).

Fields of normalized temperatures are shown in Figures 11–14. Figures 11 and 12 represent temperature fields on plain sheet. Figure 11 shows experimental results and Figure 12 shows results obtained by numerical simulation. Figures 13 and 14 represent temperature fields on hexagonal sheet. Figure 13 shows experimental results and Figure 14 shows results obtained by numerical simulation. Results show highest temperature regions near the rear side of sheets in terms of airflow direction. This proves that the heat transfer is more intense in front parts of the sheets. It is given by the lower temperature difference on the rear part of sheets and also by the airflow separation observed near the rear parts of sheets. Difference between temperature distribution in experimental and numerical results is partly caused by simplified input heat profile used for numerical simulations. Results for hexagonal sheet showed that the maximum temperature is in the rear half of every hexagon. This effect occurred on both experimental and numerical results. Figure 15 shows velocity distribution and vector velocity depictions in the space between two hexagons. The small vortex was formed in this area which can contribute to the higher heat transfer

intensity. However, this vortex can be observed only at the beginning of sheet in meaning of flow direction. After half of sheet length, the complex flow around the structured sheet was created as it is depicted in Figures 16 and 17. The Figure 16 shows temperature distribution on the part of a hexagonal sheet outlet crosswise to flow direction. Figure 17 captures the same area but shows the velocity field. There was a strong vertical flow which influenced further the heat transfers. The fact that the heat transfer intensity changed dramatically at the second part of the sheet was detectable from the temperature measurement and was also confirmed numerically. The previous study of the heat transfer intensity carried out for various structured metal plates [3] revealed the similar effect of the flow character around the surfaces.

7 Conclusions

The experimental facility was designed and constructed for the purpose of testing heat transfer intensity for arbitrary structures on metal sheet surface under different airflow and heat conditions. Methods for measurements of leading quantities were described. The heat transfer intensity between surfaces of sheets and surrounding airflow was investigated numerically and experimentally. Numerical and experimental results confirmed expected trends between plain and structured sheets in respect to the heat transfer intensity. The surface temperature differences between plain and structured hexagonal sheets were in range from 9% (for low heat power and low Reynolds number) to 20% (for high heat power and high Reynolds number). Simultaneously, numerical methods were studied for these types of simulations. Obtained numerical results were in a good match with experimental results. Small deviations were caused by inhomogeneous heat distribution over the sheet, inhomogeneous velocity field above the sheet, estimated boundary conditions settings and inaccuracy caused by the weakness of the turbulence model. The results showed some benefits of using hexagonal sheets against the plain sheets. The method of testing presented in this study could be used for different surface structures for comparison and also for development of better structures for heat shields in automotive. In future, the different structures will be tested and more accurate turbulent model will be sought.

Acknowledgments

This work is dedicated to specific research project at the Faculty of Mechanical Engineering no. 117.

References

- [1] M. Mirtsch and A. Yadav. (2006). Structured sheet metal – Part I. *Stamping Journal*. [Online]. Available: <http://www.thefabricator.com/article/metalsmaterials/structured-sheet-metal---part-i>
- [2] M. Mirtsch and A. Yadav. (2006). Structured sheet metal – Part II. *Stamping Journal*. [Online]. Available : <http://www.thefabricator.com/article/metalsmaterials/structured-sheet-metal---part-ii>
- [3] K. Fraña and S. Simon, “Air Flows along Perforated Metal Plates with the Heat Transfer,” *International Journal of Mechanical*, vol. 9, no. 8, pp. 1517–1522, 2015.
- [4] R. L. Webb and N. KIM, *Principles of enhanced heat transfer*, 2nd ed. Boca Raton: Taylor & Francis, 2005.
- [5] T. Kuppan, *Heat exchanger design handbook*, 2nd ed. Boca Raton, FL: CRC Press, 2013.
- [6] Aluminized steels. (2016 Mar. 25). *ArcelorMittal*. [online]. Available: http://automotive.arcelormittal.com/saturnus/sheets/T_EN.html
- [7] F. Kazak, *Experimentelle Charakterisierung von strukturierten Blechen unter statischen und schwingenden Belastungen*. Aachen: Shaker, 2015.
- [8] V. Malikov, *Experimentelle und numerische Untersuchungen der Umformung von strukturierten Blechen*. Berlin: Winter-Industries GmbH, 2013.
- [9] R. L. Webb and N. KIM, *Principles of enhanced heat transfer*, 2nd ed. Boca Raton: Taylor & Francis, 2005.